Contribution from the Departments of Chemistry, University of Georgia, Athens, Georgia 30602, and Emory University, Atlanta, Georgia 30322, and Department of Physics, University of Illinois, Urbana, Illinois 61801

(μ-Oxo/hydroxo)bis(μ-carboxylato)diiron(III) and -dimanganese(III) Complexes with Capping Tris(imidazol-2-yl)phosphine Ligands

Feng-Jung Wu,[†] Donald M. Kurtz, Jr.,*[,†] Karl S. Hagen,[‡] Philip D. Nyman,[§] Peter G. Debrunner,[§] and Vivian A. Vankai[†]

Received May 18, 1990

Reported are the syntheses and characterizations of the first examples of (μ-oxo/hydroxo)bis(μ-carboxylato)diiron(III) and -dimanganese(III) cores containing capping tridentate imidazolyl ligands. The capping ligands are tris(imidazol-2-yl)phosphine (TIP) and tris(*N*-methylimidazol-2-yl)phosphine (TMIP). $[Fe_2O(OAc)_2(TMIP)_2](ClO_4)_2\cdot 3CH_3CN\cdot(C_2H_5)_2O$ (OAc = acetato(1-)) crystallizes in the monoclinic space group $P2_1/c$, with $Z = 4$, $a = 12.490$ (4) Å, $b = 25.654$ (12) Å, $c = 16.909$ (9) Å, $\beta = 90.11$ (4)°, $V = 5418$ (4) Å^3, $R = 0.057$, and $R_w = 0.062$. The average Fe–O_{oxo} bond distance is 1.800 (5) Å, the Fe–O_{oxo}–Fe angle is 122.7 (2)°, and the intramolecular Fe···Fe distance is 3.158 (2) Å. The two Fe–N_{Im} bond distances trans to the oxo bridge are an average of 0.03 Å longer than the four cis Fe–N_{Im} bond distances. The iron atoms in $[Fe_2O(O_2CC_2H_5)_2(TMIP)_2](PF_6)_2\cdot CH_3CN$ are antiferromagnetically coupled, $\hat{H}_{ex} = -2J\hat{S}_1\cdot\hat{S}_2$, $S_1 = S_2 = {}^5/_2$ with $-J = 120$ cm^{-1}. For the hydroxo-bridged complexes, $[Fe_2(OH)(OAc)_2(TMIP)_2](ClO_4)_2BF_4$ and $[Fe_2(OH)(O_2CC_2H_5)_2(TMIP)_2](ClO_4)_3$, $-J \sim 17$ cm^{-1} was estimated from ^{1}H NMR isotropic shifts and a room-temperature magnetic moment. The ^{57}Fe Mössbauer quadrupole splitting for the latter hydroxo-bridged complex (0.51 mm/s) shows a pronounced decrease compared to that of the oxo-bridged complexes (1.6 mm/s). These results confirm previous interpretations of ^{1}H NMR spectra of these diiron complexes in terms of their structures and magnetic properties (Wu, F.-J.; Kurtz, D. M., Jr. *J. Am. Chem. Soc.* **1989**, *111*, 6563). The isostructural dimanganese(III) complex, $[Mn_2O(OAc)_2(TMIP)_2](ClO_4)_2\cdot 2CH_3CN\cdot 0.5(C_2H_5)_2O$, crystallizes in the orthorhombic space group *Pnaa* with $Z = 8$, $a = 13.545$ (4) Å, $b = 22.285$ (15), Å, $c = 33.47$ (3) Å, $V = 10101$ (12) Å^3, $R = 0.087$, and $R_w = 0.089$. The average Mn–O_{oxo} bond distance is 1.789 (11) Å, the Mn–O_{oxo}–Mn angle is 124.4 (6)°, and the intramolecular Mn···Mn distance is 3.164 (5) Å. Bond lengthening along one set of N–Mn–O_{OAc} axes on each Mn atom is consistent with unoccupied d_{z^2} orbitals along the Mn–O_{oxo} axes. These unoccupied orbitals are reflected in extremely weak antiferromagnetic coupling ($-J \leq 0.5$ cm^{-1}) and in the pattern of isotropic shifts observed for ^{1}H NMR resonances of imidazolyl ligands that are cis and trans to the oxo bridge. These complexes provide structural and spectroscopic benchmarks for imidazole-containing oxo/hydroxo-bridged diiron(III) and dimanganese(III) sites in non-heme proteins such as hemerythrin, ribonucleotide reductase, and pseudocatalase.

The tribridged structural category of (μ-oxo/hydroxo)diiron complexes was introduced in 1983 with the syntheses of two (μ-oxo)bis(μ-carboxylato)diiron(III) "hemerythrin site models" independently in the laboratories of Lippard[1] and Wieghardt.[2] These diiron(III) complexes form by "spontaneous self-assembly" using a variety of tridentate (usually N-donor) ligands that cap each end of the (μ-oxo)bis(μ-carboxylato)diiron(III) core.[3] As implied by the connection to hemerythrin, these syntheses were driven largely by attempts to understand the chemistry of an emerging group of diiron sites in proteins.[4] A parallel structural chemistry has more recently arisen for tribridged (μ-oxo/hydroxo)dimanganese complexes.[5,6] In this case too, the structural chemistry appears to mimic biology. Thus, these (μ-oxo)diiron and -dimanganese complexes provide structural and spectroscopic benchmarks for dimetal sites in proteins such as hemerythrin,[4] ribonucleotide reductase,[4,7] and pseudocatalase.[6,8] Imidazolyl side chains of histidine residues are known to furnish a total of five ligands to the diiron site in hemerythrin (cf. Chart I) and are strongly suspected to furnish ligands to diiron and dimanganese sites in the other proteins listed above.

In a recent ^{1}H NMR study of iron–imidazole complexes, Wu and Kurtz[9] reported the first examples of tridentate imidazolyl capping ligands on the (μ-oxo/hydroxo)bis(μ-carboxylato)diiron(III) core.[10] They used the tris(imidazol-2-yl)phosphines TIP and TMIP[12] (see Chart I) to prepare the oxo-bridged complexes $[Fe_2O(OAc)_2L_2]^{2+}$ (L = TIP and TMIP) and $[Fe_2O(OPr)_2(TMIP)_2]^{2+}$ and the hydroxo-bridged complexes $[Fe_2(OH)(OAc)_2(TMIP)_2]^{3+}$ and $[Fe_2(OH)(OPr)_2(TMIP)_2]^{3+}$. The resonance Raman spectrum of $[Fe_2O(OPr)_2(TMIP)_2]^{2+}$ has also recently been reported.[13] These reports were unaccompanied by synthetic procedures or other characterizations of these complexes. Herein we describe the syntheses and further characterizations of these diiron(III) complexes and the extension of this chemistry to manganese(III). No tribridged (μ-oxo)dimanganese complexes containing terminal imidazolyl ligands have been previously reported.

Chart I

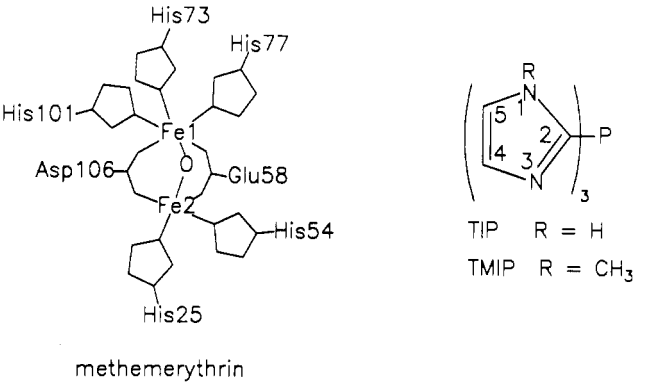

The compounds reported here also expand the coordination chemistry of tris(imidazol-2-yl)phosphine ligands, which in the

[†] University of Georgia.
[‡] Emory University.
[§] University of Illinois.

(1) Armstrong, W. H.; Lippard, S. J. *J. Am. Chem. Soc.* **1983**, *105*, 4837.
(2) Wieghardt, K.; Pohl, J.; Gebrt, W. *Angew. Chem., Int. Ed. Engl.* **1983**, *22*, 727.
(3) Kurtz, D. M., Jr. *Chem. Rev.* **1990**, *90*, 585.
(4) (a) Que, L., Jr.; Scarrow, R. C. In *Metal Clusters in Proteins*; Que, L., Jr., Ed.; ACS Symposium Series 372; American Chemical Society: Washington, DC, 1988; p 152. (b) Sanders-Loehr, J. In *Iron Carriers and Iron Proteins*, Loehr, T. M., Ed.; VCH: New York, 1989; p 373.
(5) (a) Sheats, J. E.; Czernuszewicz, R. S.; Dismukes, G. C.; Rheingold, A. L.; Petrouleas, V. L.; Stubbe, J.; Armstrong, W. H.; Beer, R. H.; Lippard, S. J. *J. Am. Chem. Soc.* **1987**, *109*, 1435. (b) Wieghardt, K.; Bossek, U.; Nuber, B.; Weiss, J.; Bonvoisin, J.; Corbella, M.; Vitols, S. E.; Girerd, J. J. *J. Am. Chem. Soc.* **1988**, *110*, 7398. (c) Wieghardt, K.; Bossek, V.; Ventur, D.; Weiss, J. *J. Chem. Soc., Chem. Commun.* **1985**, 347.
(6) Wieghardt, K. *Angew. Chem., Int. Ed. Engl.* **1989**, *28*, 1153.
(7) Willing, A.; Follman, H.; Auling, G. *Eur. J. Biochem.* **1988**, *170*, 603.
(8) Fronko, R. M.; Penner-Hahn, J. E.; Bender, C. J. *J. Am. Chem. Soc.* **1988**, *110*, 7554.
(9) Wu, F.-J.; Kurtz, D. M., Jr. *J. Am. Chem. Soc.* **1989**, *111*, 6563.
(10) Capping benzimidazolyl ligands on this core have been reported.[11]
(11) (a) Gomez-Romero, P.; Casan-Pastor, N.; Ben-Hussein, A.; Jameson, G. B. *J. Am. Chem. Soc.* **1988**, *110*, 1988. (b) Nishida, Y.; Haga, S.; Tokii, T. *Chem. Lett.* **1989**, 109. (c) Adams, H.; Bailey, N. A.; Crane, J. D.; Fenton, D. E.; Latour, J.-M.; Williams, J. M. *J. Chem. Soc., Dalton Trans.* **1990**, 1727.

0020-1669/90/1329-5174$02.50/0

past has been limited to Zn(II) and Co(II).[14] A 1:1 tris(4,5-diisopropylimidazol-2-yl)phosphine/zinc(II) complex has been structurally characterized, and shows tridentate chelation through the three imidazolyl-N(3) atoms.[15] The related tris(pyrid-2-yl)phosphines have been reported to form simple bis(ligand) complexes with a variety of divalent transition metals, including iron.[16] In all cases, the evidence favors coordination exclusively through nitrogen lone pairs, usually in a tridentate fashion; there is currently no evidence for coordination through phosphorus with either the tris(pyridyl)- or tris(imidazolyl)phosphine ligands.

Experimental Section

Materials and Methods. Preparations of Compounds. Solvents and reagents were obtained mainly from Aldrich Chemical Co. and used without further purification unless otherwise noted. Acetonitrile and methylene chloride were distilled from CaH_2. Ethyl ether was distilled from sodium/benzophenone. $(Et_4N)_2[Fe_2OCl_6]$[17] and TIP[18] were prepared by previously described procedures.

TMIP. This ligand was synthesized according to the procedure described for TIP[18] but with *N*-methylimidazole in place of *N*-(diethoxymethyl)imidazole and with the following modifications. During the two-phase extraction with ethyl ether/water, TMIP was found to be extracted into the water rather than ether phase. The water phase was separated from the ether phase and then extracted three times with an equal volume of dichloromethane. After removal of the dichloromethane, the residue was recrystallized from toluene or toluene/hexanes. The yield was ~40% as a light yellow solid. ^1H NMR: *N*-CH_3, 3.62 ppm; 4,5-H, 7.07, 7.19 ppm.

The reactions described below in aqueous solutions were performed aerobically. Reactions in organic solvents and workup of products were normally performed under N_2 or Ar by using Schlenk-type glassware and vacuum-line manipulations. Elemental analyses were performed by Atlantic Microlabs, Inc., Atlanta, GA. Molecules of solvation were inferred from elemental analyses and for two compounds were located by X-ray crystallography.

$[Fe(TIP)_2](ClO_4)_3\cdot 3H_2O$. $Fe(ClO_4)_3\cdot 6H_2O$ (1.80 g, 3.88 mmol) and sodium acetate trihydrate (1.05 g, 7.76 mmol) were mixed in 30 mL of H_2O. To the resulting deep orange solution was added 0.60 g (2.59 mmol) of solid TIP. This solid dissolved gradually and a precipitate formed after a few minutes. After 30 min of stirring, the deep orange-red suspension was filtered. The deep brown precipitate was filtered, washed with ethanol and ethyl ether, and then pumped to dryness. The yield was 0.60 g (53%). Anal. Calcd for $C_{18}H_{24}N_{12}FeCl_3O_{15}P_2$: C, 24.78; H, 2.77; N, 19.26; Cl, 12.19. Found: C, 25.05; H, 2.83; N, 19.22, Cl, 12.23. ^1H NMR spectrum (CD_3CN): see ref 9. *Warning! A small amount of solid $[Fe(TIP)_2](ClO_4)_3\cdot \le 3H_2O$ detonated violently while being scraped from a glass frit with a stainless-steel spatula. While we have noted no such behavior for any of the perchlorate salts described below, all perchlorate salts should be handled with caution.*

$[Fe(TMIP)_2](ClO_4)_3$. This compound was prepared in a manner analogous to that used for the TIP-containing salt and identified by comparison of its ^1H NMR spectrum (given in ref 9) with that of $[Fe(TIP)_2](ClO_4)_3\cdot 3H_2O$.

$[Fe_2O(OAc)_2(TIP)_2](ClO_4)_2\cdot H_2O$. To 35 mL of an aqueous solution containing 3.39 (5.17 mmol) of $Fe(ClO_4)_3\cdot 6H_2O$ and 1.76 g (12.9 mmol) of sodium acetate trihydrate (pH 4.1) was added 18.15 g (129 mmol) of $NaClO_4\cdot H_2O$, which raised the pH to 4.25 and gave a clear orange-red solution. TIP (0.60 g, 2.58 mmol) was dissolved in ~15 mL of HPLC grade methanol. Dropwise addition of this methanol solution to the orange-red aqueous solution over the course of ~3 min with vigorous stirring resulted in the gradual formation of a green suspension. This suspension was filtered after about 10 min of rapid stirring (filtrate pH 4.9). The bright green solid on the frit was freed of $NaClO_4$ by washing consecutively with small volumes (2–3 mL) of cold methanol, cold ethanol, and ethanol/ethyl ether and finally with 3 × 10 mL ethyl ether. This purification step resulted in a considerable loss of the desired product. The solid was then pumped to dryness in vacuo. The yield was 30–50% and was highly dependent on pH, rapid removal of the desired product from the aqueous reaction mixture, and the subsequent workup. Recrystallization from acetonitrile/ethyl ether gave analytically pure material. Anal. Calcd for $C_{22}H_{26}N_{12}Cl_2Fe_2O_{14}P_2$: C, 28.51; H, 2.81, N, 18.14. Found: C, 28.72; H, 3.30; N, 18.04. ^1H NMR (CD_3CN): see ref 9.

$[Fe_2O(OAc)_2(TMIP)_2](ClO_4)_2\cdot CH_3CN$. To a clear deep red solution of $Fe(ClO_4)_3\cdot 6H_2O$ (5.32 g, 11.5 mmol) and sodium acetate trihydrate (3.91 g, 28.8 mmol) in 120 mL of water (pH 3.2) was added with stirring a solution of TMIP (3.15 g, 11.5 mmol) in 30 mL of water. The resulting green suspension was filtered after 5 h of stirring (filtrate pH 4.8), and the green solid was dried in vacuo after washing with 50 mL of ethyl ether. This green solid was shown by ^1H NMR and UV–vis spectroscopies to be $[Fe_2O(OAc)_2(TMIP)_2](ClO_4)_2$ contaminated with about 14 mol % of $[Fe(TMIP)_2](ClO_4)_3$. This solid was recrystallized from acetonitrile/ethyl ether to give the pure compound as green needles (yield, 2.8 g, 53%). $[Fe(TMIP)_2](ClO_4)_3$ was found to much less soluble than $[Fe_2O(OAc)_2(TMIP)_2](ClO_4)_2$ in acetonitrile/ether. The sample used for elemental analysis was pumped to dryness in vacuo, which, on the basis of the elemental analysis, removed two of the three acetonitrile solvate molecules per cation found in the X-ray crystal structure (vide infra). Anal. Calcd for $C_{30}H_{39}N_{13}Cl_2Fe_2O_{13}P_2$: C, 34.84; H, 3.80; N, 17.61; Fe, 10.80; Cl, 6.86. Found: C, 34.54; H, 3.84; N, 17.48; Fe, 11.06; Cl, 6.49. ^1H NMR (CD_3CN): cf. ref 9. Absorption spectral data (CH_3CN λ_{max}, nm (ϵ, M^{-1} cm^{-1}): 338 (7900), 360 sh (6900), 455 (1060), 492 (940), 536 sh (150), 705 (110).

$[Fe_2O(OPr)_2(TMIP)_2](PF_6)_2\cdot CH_3CN$. $(Et_4N)_2[Fe_2OCl_6]$ (0.99 g, 1.65 mmol) and sodium propionate (0.40 g, 4.2 mmol) were combined in 30 mL of acetonitrile and stirred for 30 min. To the resulting deep red-brown suspension were added 1.21 g (6.6 mmol) of KPF_6 and 0.90 g (3.3 mmol) of TMIP. A greenish brown suspension gradually formed. The reaction mixture was stirred for 90 min and filtered to remove a white solid, and the solvent was removed from the filtrate in vacuo. The greenish brown residue was triturated with 30 mL of methanol to remove Et_4NPF_6. Filtration and drying afforded a bright green crude product, which ^1H NMR showed to be contaminated by small amounts of $[Fe(TMIP)_2](PF_6)_3$ and Et_4NPF_6. This crude product was recrystallized from acetonitrile/ethyl ether at −20 °C, $[Fe(TMIP)_2](PF_6)_3$ being much less soluble in this medium. The yield of the title compound was 0.90 g (48%), assuming one acetonitrile of crystallization. Anal. Calcd for $C_{32}H_{43}N_{13}F_{12}Fe_2P_4$: C, 33.33; H, 3.73; N, 15.79; Fe, 9.68; F, 19.77. Found: C, 33.42; H, 3.25; N, 15.40; Fe, 9.97; F, 19.23. ^1H NMR (CD_3CN): see ref 9. Resonance Raman: see ref 13. Absorption spectral data (CH_3CN λ_{max}, nm (ϵ, M^{-1} cm^{-1})): 339 (6×10^3), 361 sh, 460 (890), 494 (810), 702 (130).

$[Fe_2(OH)(OPr)_2(TMIP)_2](ClO_4)_3\cdot CH_3CN\cdot H_2O$. To a clear orange-red solution of $Fe(ClO_4)_3\cdot 6H_2O$ (2.02 g, 4.38 mmol) and sodium propionate (0.84 g, 8.75) in 20 mL of water (pH 2.2) was added diluted perchloric acid (~8 mL) until a pH of 1.5 was obtained. TMIP (0.61 g, 2.2 mmol) in 10 mL of water was then added to the solution, and a yellow precipitate formed immediately. After 10 min of vigorous stirring, the suspension was filtered (filtrate pH 1.7), and the yellow solid was washed successively with ethanol (2 × 5 mL), 1:1 (v/v) ethanol/ethyl ether (20 mL), and ethyl ether (2 × 20 mL). After being dried in vacuo, this yellow solid, shown by ^1H NMR to be contaminated by a trace of $[Fe(TMIP)_2](ClO_4)_3$, was recrystallized from the ethyl ether/acetonitrile either at −20 °C or by vapor diffusion to afford (after removal of less soluble $[Fe(TMIP)_2][ClO_4)_3$ and an unidentified white solid) the title compound as orange crystals in 55% yield. The analysis was consistent with one acetonitrile and one water of crystallization. Anal. Calcd for $C_{32}H_{46}N_{13}Fe_2Cl_3O_{18}$ C, 32.55; H, 3.93; N, 15.42; Fe, 9.46; Cl, 9.01. Found: C, 32.77; H, 4.11; N, 15.38; Fe, 9.38; Cl, 8.64. ^1H NMR spectrum (CD_3CN): see ref 9.

$[Fe_2(OH)(OAc)_2(TMIP)_2](ClO_4)_2BF_4$. This compound was prepared in situ by addition of 1 equiv of $HBF_4\cdot O(C_2H_5)_2$ to a solution of $[Fe_2O(OAc)_2(TMIP)_2](ClO_4)_2\cdot CH_3CN$ in acetonitrile. Completeness of reaction and lack of appreciable conversion to $[Fe(TMIP)_2](ClO_4)_3$ was ascertained by ^1H NMR. ^1H NMR spectrum (CD_3CN): see ref 9.

$[Mn_2O(OAc)_2(TMIP)_2](PF_6)_2$. Manganese(III) acetate dihydrate (0.80 g, 3.0 mmol) and KPF_6 (0.55 g, 3.0 mmol) in 70 mL of degassed acetonitrile were stirred for 40 min, resulting in a brown-black suspension. TMIP (0.82 g, 3 mmol) was then added to the suspension, and the

(12) Abbreviations used: TIP, tris(imidazol-2-yl)phosphine; TMIP, tris(*N*-methylimidazol-2-yl)phosphine; OAc, acetate(1−); OPr, propionate(1−); TACN, 1,4,7-triazacyclononane; MTACN, *N,N',N''*-trimethyl-1,4,7-triazacyclononane; TICOH, tris(*N*-methylimidazol-2-yl)hydroxymethane; TICOMe, 1,1,1-tris(*N*-methylimidazol-2-yl)methyl ether; Et_4N, tetraethylammonium cation; $HB(pz)_3$, tris(1-pyrazolyl)hydroborate(1−); MPDP, *m*-phenylenedipropionate(2−).

(13) Sanders-Loehr, J.; Wheeler, W. D.; Shiemke, A. K.; Averill, B. A.; Loehr, T. M. *J. Am. Chem. Soc.* **1989**, *111*, 8084.
(14) (a) Brown, R. S.; Zamkanei, M.; Cocho, J. L. *J. Am. Chem. Soc.* **1984**, *106*, 5222. (b) Brown, R. S.; Curtis, N. J.; Huguet, J. *J. Am. Chem. Soc.* **1981**, *103*, 6953.
(15) Read, R. J.; James, M. N. G. *J. Am. Chem. Soc.* **1981**, *103*, 6947.
(16) (a) Boggess, R. K.; Zatko, D. A. *J. Coord. Chem.* **1975**, *4*, 217. (b) Boggess, R. K.; Zatko, D. A. *Inorg. Chem.* **1976**, *15*, 626. (c) Boggess, R. K.; Hughes, J. W.; Chew, C. W.; Kemper, J. J. *J. Inorg. Nucl. Chem.* **1981**, *43*, 939.
(17) Armstrong, W. H.; Lippard, S. J. *Inorg. Chem.* **1985**, *24*, 981.
(18) Curtis, N. J.; Brown, R. S. *J. Org. Chem.* **1980**, *45*, 4038.

mixture was stirred for 90 min. The solution/suspension gradually turned purple, as the TMIP dissolved. The reaction mixture was filtered to remove a brown solid. Solvent was removed from the purple filtrate, and the purple residue was washed with 20 mL of ethyl ether. Several recrystallizations of this residue from acetonitrile/ethyl ether at −20 °C (sometimes accompanied by formation of a less-dense white solid) afforded the title compound (0.35 g, 11%) as purple needles. Anal. Calcd for $C_{28}H_{36}N_{12}F_{12}Mn_2O_5P_4$: C, 31.07; H, 3.35; N, 15.53; Mn, 10.15. Found: C, 31.19; H, 3.39, N, 15.29; Mn, 10.05. Absorption spectral data (CH_3CN λ_{max}, nm (ϵ, M^{-1} cm^{-1})): 249 (24 900), 372 sh (840), 464 sh (360), 485 (460), 502 (430), 521 sh (400), 568 sh (240), 757 (130). ^1H NMR (CD_3CN at ~23 °C, δ in ppm): 66, 49, 22, 20, 12, −4, −44.

$[Mn_2O(OAc)_2(TMIP)_2](ClO_4)_2 \cdot 2CH_3CN$. Manganese(III) acetate dihydrate (0.98 g, 3.7 mmol) and $NaClO_4 \cdot H_2O$ (0.51 g, 3.7 mmol) were stirred in 20 mL of acetonitrile for 45 min. TMIP (1.09 g, 3.64 mmol) was added as a solid, and the suspension was stirred for 90 min during which time a purple color developed. The mixture was filtered, and the filtrate was evaporated to dryness *in vacuo*. The residue was dissolved in 15 mL of acetonitrile, and 15 mL of ethyl ether was added. Storage of this solution at −20 °C resulted in the formation of purple crystals. These crystals were washed with ethyl ether, pumped to dryness in vacuo, and recrystallized from acetonitrile/ether. The crystals were pumped to dryness prior to elemental analysis, which apparently removed most of the ethyl ether solvate found in the X-ray crystal structure (vide infra). No ethyl ether was evident in the ^1H NMR spectrum of crystals which had been dried in vacuo. Yield: 0.69 g (35%). Anal. Calcd for $C_{32}H_{42}N_{14}Cl_2Mn_2O_{13}P_2$: C, 35.78; H, 3.91; N, 18.26. Found: C, 35.85; H, 4.05; N, 17.86. Absorption spectrum (CH_3CN λ_{max}, nm (ϵ, M^{-1} cm^{-1})): 255 (23,900), 376 (844), 464 (330), 484 (405), 497 (383), 521 sh (349), 568 sh (216), 736 (106). ^1H NMR: identical with that of given above for the analogous PF_6^- salt.

Physical Measurements. ^1H NMR spectra and solution magnetic moments were measured as described previously.[9] NMR chemical shifts were referenced to $(CH_3)_4Si$ at 300 K. Downfield and upfield shifts are reported as positive and negative, respectively. Electronic absorption spectra were obtained on a Perkin-Elmer Model 3840 λ-array spectrophotometer. Cyclic voltammetry was performed on N_2-purged solutions in acetonitrile that contained 0.1 M tetrabutylammonium hexafluorophosphate as supporting electrolyte. For these electrochemical measurements, a Bioanalytical Systems Model 100 electrochemical analyzer was equipped with a platinum-disk working electrode and an Ag/AgCl reference electrode. A scan rate of 100 mV/s was used. Mössbauer data were recorded on powder samples in transmission, using a conventional constant acceleration spectrometer in conjunction with a Janis Varitemp helium flow cryostat. The data were least-squares fitted by Lorenztians;[19] all isomer shifts are quoted relative to that of iron foil at 300 K. Magnetic moments were measured on a SHE VTS-50 SQUID susceptometer at temperatures from 4 to 300 K and fields up to 4.5 T. Circa 150 mg of the powdered samples were placed in a quartz bulb or a gelatine capsule (Lilly). No paramagnetic corrections were needed; diamagnetic corrections were significant for $[Fe_2O(OPr)_2(TMIP)_2](PF_6)_2 \cdot CH_3CN$ only.

X-ray Data Collection, Reduction, Solution, and Refinement. Crystals of $[M_2O(OAc)_2(TMIP)_2](ClO_4)_2$ (M_2 = $Fe_2(\cdot 3CH_3CN \cdot (C_2H_5)_2O)$, $Mn_2(\cdot 2CH_3CN \cdot 0.5(C_2H_5)_2O)$) were grown by ether diffusion into acetonitrile solutions of the compounds. Crystals used for X-ray crystallography were not pumped to dryness in contrast to the synthetic procedures described above. Crystals of the iron compound were found to lose solvent rapidly and were, therefore, cooled to −80 °C on a microscope stage for examination and crystal mounting. The green crystal, mounted on a glass fiber with "super-glue" was transferred rapidly to the cold stream on a NicoletP3F four-circle diffractometer and maintained at −75 °C. Both monoclinic and orthorhombic forms of the manganese compound formed, and (since they were more stable) the purple crystals were mounted on a fiber and completely coated with "super-glue". The orientation matrix and unit cell dimensions were calculated by least-squares treatment of 25 machine-centered reflections ($20° < 2\theta < 25°$) obtained by using graphite-monochromatized Mo Kα radiation. Crystallographic details are given in Tables I and SI. Three check reflection intensities were measured every 123 reflections and exhibited no decay. The data were processed with the program XTAPE of the SHELXTL program package (Siemens Analytical X-Ray Instruments, Inc., Madison, WI); no absorption correction was applied to the data. Systematic absences *h0l* ($l = 2n + 1$) and *0k0* ($k = 2n + 1$) uniquely defined the space group $P2_1/c$ for the monoclinic forms and *0kl* ($k + l = 2n + 1$), and *hk0* ($h = 2n + 1$), *h0l* ($h = 2n + 1$), and *hk0* ($h = 2n + 1$) uniquely defined the space group as *Pnaa* (nonstandard setting of *Pccn*) for the orthorhombic manganese crystal. For the iron compound, the positions of all non-hydrogen atoms of the cation and one anion were obtained from a Patterson interpretation and structure expansion using SHELXS-86.[20a] For the manganese compound, the Mn, P, and Cl atoms were located by SHELXS-86. The remaining non-hydrogen atoms were found by successive difference Fourier maps and least-squares refinement using SHELX-76[20b] and SHELXTL programs. Neutral-atom scattering factors with anomalous dispersion corrections were used throughout.[21] For the iron compound all non-hydrogen atoms were refined with anisotropic thermal parameters, whereas for the manganese compound only selected non-hydrogen atoms were refined anisotropically due to the lower number of observed data points. Fixed contributions from hydrogen atoms were included with a C–H distance of 0.96 Å and thermal parameter set at 1.2 times that of the bonded carbon atom. No significant electron density was left unaccounted for, the largest being 0.8 $e^-/Å^3$ in the difference Fourier map of the manganese compound. Final *R* factors are given in Table I. The following results are tabulated: positional and thermal parameters (Tables II, III, SIII, and SVI), interatomic distances and angles (Tables IV, SVIII, and SX), anisotropic thermal parameters (Tables SII and SV), and values of $10|F_o|$ and $10|F_c|$ (Tables SXI and SXII).

Table I. Crystallographic Data for $[M_2O(OAc)_2(TMIP)_2](ClO_4)_2$ (M_2 = $Fe_2(\cdot 3CH_3CN \cdot (C_2H_5)_2O)$, $Mn_2(\cdot 2CH_3CN \cdot 0.5(C_2H_5)_2O)$)

formula	$C_{38}Cl_2Fe_2H_{55}N_{15}O_{13}P_2$	$C_{34}Cl_2H_{47}Mn_2N_{14}O_{13.5}P_2$
fw	1174.5	1176.0
a, Å	12.490 (4)	13.545 (4)
b, Å	25.654 (12)	22.285 (15)
c, Å	16.909 (9)	33.47 (3)
β, deg	90.11 (4)	
Vol, Å^3	5418 (4)	10101 (12)
space group (No.)	$P2_1/c$ (14)	*Pnaa* (56)
d_{calcd}, g/cm$_3$	1.44	1.38
Z	4	8
temp, °C	−75	21
radiation	Mo Kα (λ = 0.710 73 Å)	
abs coeff (μ), cm^{-1}	7.6	7.1
R, %	5.7	8.7
R_w, %	6.2	8.9

Results and Discussion

Syntheses. Syntheses of the (μ-oxo)bis(μ-carboxylato)diiron(III) complexes with tris(imidazol-2-yl)phosphines as capping ligands used either one of two procedures that have become standard for such complexes.[3] These methods are (i) combination of ferric perchlorate and sodium acetate in water followed by addition of tridentate ligand or (ii), for less water-soluble carboxylates, mixing of $[Fe_2OCl_6]^{2-}$ with NaO_2CR in acetonitrile followed by addition of capping ligand. Much greater difficulty was encountered with TIP than with TMIP in synthesizing the dinuclear complexes. Only the aqueous procedure gave the desired product with TIP. The yield of $[Fe_2O(OAc)_2(TIP)_2](ClO_4)_2$ (30–50%) was found to be critically dependent on pH and on rapid removal of the desired product from the aqueous reaction mixture. The pH was determined by the ratio of ferric perchlorate to sodium acetate, both of which were present in large excess over TIP. A lower pH than specified in the experimental procedure resulted in contamination with $[Fe(TIP)_2](ClO_4)_3$. This latter salt was the only isolable product in the absence of a large excess of perchlorate, which favors precipitation of the dinuclear complexes. Vigorous stirring and gradual addition of TIP were also found to be necessary, apparently to avoid locally high concentrations of TIP. We have been unable to find conditions for isolation of the corresponding (μ-hydroxo)bis(μ-carboxylato)diiron(III) complex with TIP in either aqueous or organic solvents.

Experimental conditions were not so critical for syntheses of the analogous TMIP-containing complexes. With TMIP both (μ-oxo)- and (μ-hydroxo)bis(μ-carboxylato)diiron(III) complexes are obtainable in ~50% yields by using the two methods listed

(19) Chrisman, B. L.; Tumillilo, T. A. *Comput. Phys. Commun.* **1971**, *2*, 322.

(20) (a) Sheldrick, G. M. SHELXS-86. Program for Crystal Structure Determination, 1986. (b) Sheldrick, G. M. SHELX-76. Program for Crystal Structure Determination. University of Cambridge, Cambridge, England, 1976.

(21) *International Tables for X-ray Crystallography*; Kynoch Press: Birmingham, England, 1974; Vol. 4, pp 99, 149.

Table II. Atomic Coordinates (×10⁴) and Thermal Parameters (Å² × 10³) for $[Fe_2O(OAc)_2(TMIP)_2](ClO_4)_2 \cdot 3CH_3CN \cdot (C_2H_5)_2O$

	x	y	z	U[a]
Fe(1)	2152 (1)	1822 (1)	3637 (1)	25 (1)
Fe(2)	535 (1)	2715 (1)	3163 (1)	26 (1)
O(1)	1388 (4)	2394 (2)	3872 (3)	27 (2)
O(2)	943 (4)	1440 (2)	3050 (3)	32 (2)
O(3)	−231 (4)	2068 (2)	2757 (3)	36 (2)
C(1)	68 (6)	1596 (3)	2766 (4)	28 (2)
C(2)	−675 (6)	1206 (3)	2418 (5)	43 (3)
O(4)	2803 (4)	2102 (2)	2616 (3)	35 (2)
O(5)	1591 (4)	2704 (2)	2245 (3)	33 (2)
C(3)	2477 (6)	2479 (3)	2191 (4)	29 (2)
C(4)	3263 (6)	2669 (3)	1570 (4)	43 (3)
P(1)	3884 (2)	1022 (1)	4885 (1)	27 (1)
N(11)	3003 (5)	1096 (2)	3370 (3)	30 (2)
C(11)	3615 (5)	826 (3)	3869 (4)	26 (2)
N(21)	3978 (5)	389 (2)	3530 (3)	31 (2)
C(21)	2985 (6)	816 (3)	2681 (4)	37 (3)
C(31)	3583 (6)	379 (3)	2773 (4)	38 (3)
C(41)	4668 (6)	−9 (3)	3871 (4)	35 (3)
N(31)	1795 (4)	1422 (2)	4736 (3)	25 (2)
C(51)	2504 (6)	1157 (2)	5168 (4)	26 (2)
C(61)	889 (6)	1469 (3)	5185 (4)	31 (3)
C(71)	1050 (6)	1228 (3)	5892 (4)	37 (3)
N(41)	2071 (5)	1030 (2)	5876 (3)	28 (2)
C(81)	2596 (6)	758 (3)	6529 (4)	35 (3)
N(51)	3635 (4)	2022 (2)	4233 (4)	31 (2)
C(91)	4194 (5)	1707 (3)	4698 (4)	26 (2)
C(101)	4108 (6)	2503 (3)	4288 (5)	39 (3)
C(111)	4930 (6)	2476 (3)	4803 (5)	43 (3)
N(61)	4996 (5)	1974 (2)	5061 (4)	33 (2)
C(121)	5749 (6)	1773 (3)	5628 (5)	46 (3)
P(2)	−1017 (2)	3904 (1)	3421 (1)	31 (1)
N(12)	−551 (4)	3109 (2)	2345 (3)	27 (2)
C(12)	−1081 (5)	3552 (3)	2489 (4)	26 (2)
C(22)	−836 (6)	2967 (3)	1594 (4)	32 (3)
C(32)	−1505 (6)	3323 (3)	1292 (4)	34 (3)
N(22)	−1669 (5)	3686 (2)	1849 (4)	28 (2)
C(42)	−2390 (6)	4130 (3)	1783 (5)	42 (3)
C(52)	−1235 (5)	3337 (3)	4049 (4)	29 (2)
N(32)	−753 (4)	2877 (2)	3971 (3)	30 (2)
C(62)	−1167 (6)	2561 (3)	4547 (5)	42 (3)
C(72)	−1897 (6)	2833 (3)	4977 (5)	45 (3)
N(42)	−1926 (5)	3320 (3)	4659 (4)	36 (2)
C(82)	−2566 (7)	3756 (3)	4965 (5)	47 (3)
C(92)	439 (6)	3906 (3)	3513 (4)	27 (2)
N(52)	1060 (4)	3490 (2)	3404 (3)	27 (2)
C(102)	2089 (6)	3655 (3)	3521 (4)	31 (3)
C(112)	2085 (6)	4173 (3)	3700 (4)	35 (3)
N(62)	1043 (5)	4323 (2)	3682 (4)	33 (2)
C(122)	649 (7)	4845 (3)	3880 (5)	48 (3)

[a] Equivalent isotropic U defined as one-third of the trace of the orthogonalized U_{ij} tensor.

Table III. Atomic Coordinates (×10⁴) and Thermal Parameters (Å² × 10³) for $[Mn_2O(OAc)_2(TMIP)_2](ClO_4)_2 \cdot 2CH_3CN \cdot 0.5(C_2H_5)_2O$

	x	y	z	U
Mn(1)	1321 (3)	380 (1)	1561 (1)	42 (1)[a]
Mn(2)	879 (2)	1193 (1)	806 (1)	48 (1)[a]
O(1)	1113 (9)	485 (4)	1035 (3)	50 (5)[a]
O(2)	2378 (10)	980 (6)	1607 (4)	69 (6)[a]
C(1)	2462 (15)	1468 (5)	1407 (5)	54 (6)
C(2)	3446 (16)	1764 (10)	1515 (7)	100 (9)
O(3)	1936 (10)	1689 (5)	1156 (3)	62 (6)[a]
O(4)	182 (10)	976 (5)	1732 (3)	62 (6)[a]
C(3)	−1382 (14)	1247 (8)	1531 (5)	44 (5)
C(4)	−1404 (16)	1431 (10)	1668 (7)	100 (9)
O(5)	−260 (10)	1402 (5)	1157 (4)	61 (6)[a]
N(11)	1489 (13)	220 (7)	2164 (4)	58 (7)[a]
P(1)	1438 (4)	−1031 (2)	2073 (2)	55 (2)[a]
C(11)	1482 (16)	−329 (9)	2346 (5)	55 (8)[a]
C(21)	1585 (13)	627 (8)	2456 (6)	54 (6)
C(31)	1639 (15)	336 (9)	2819 (6)	64 (6)
N(21)	1547 (11)	−246 (7)	2720 (4)	51 (5)
C(41)	1544 (16)	−739 (10)	3027 (6)	86 (8)
N(31)	2443 (12)	−343 (6)	1500 (4)	61 (7)[a]
C(51)	2397 (15)	−847 (9)	1711 (5)	55 (6)
C(61)	3325 (14)	−364 (10)	1298 (6)	63 (7)
C(71)	3811 (18)	−884 (10)	1376 (7)	82 (8)
N(41)	3220 (12)	−1179 (7)	1652 (5)	61 (5)
C(81)	3475 (17)	−1786 (10)	1833 (7)	98 (9)
N(51)	280 (11)	−314 (7)	1569 (4)	51 (6)[a]
C(91)	417 (15)	−819 (8)	1771 (6)	53 (6)
C(101)	−619 (15)	−349 (10)	1394 (6)	72 (7)
C(111)	−1025 (17)	−877 (10)	1475 (6)	80 (7)
N(61)	−415 (11)	−1175 (7)	1701 (4)	57 (5)
C(121)	−620 (17)	−1772 (10)	1882 (7)	92 (8)
N(12)	666 (14)	2001 (6)	513 (5)	63 (8)[a]
P(2)	831 (5)	1494 (3)	−245 (2)	65 (2)[a]
C(12)	674 (16)	2065 (8)	113 (6)	53 (9)[a]
C(22)	460 (15)	2549 (9)	671 (6)	62 (6)
C(32)	417 (18)	2958 (12)	384 (7)	91 (9)
N(22)	517 (14)	2655 (8)	31 (6)	78 (6)
C(42)	514 (19)	2932 (11)	−360 (7)	115 (10)
N(32)	1957 (11)	1042 (6)	386 (4)	55 (7)[a]
C(52)	1842 (16)	1153 (9)	−18 (6)	62 (6)
C(62)	2868 (15)	813 (9)	450 (6)	68 (7)
C(72)	3391 (17)	779 (8)	88 (6)	63 (7)
N(42)	2723 (13)	994 (7)	−185 (5)	64 (5)
C(82)	2936 (16)	1063 (10)	−615 (6)	86 (8)
N(52)	−155 (12)	823 (7)	336 (4)	55 (7)[a]
C(92)	−110 (15)	1008 (9)	−37 (6)	55 (6)
C(102)	−1011 (15)	500 (9)	370 (6)	71 (7)
C(112)	−1459 (18)	505 (9)	11 (7)	78 (7)
N(62)	−869 (14)	805 (8)	−250 (5)	72 (5)
C(122)	−1141 (17)	935 (10)	−672 (6)	91 (8)

[a] Equivalent isotropic U defined as one-third of the trace of the orthogonalized U_{ij} tensor.

above. Highest yields of the μ-hydroxo complex are obtained at a pH in the range of 1.5–2.0, compared to pH 3.5–4.5 for the μ-oxo complex. From this pH dependence, we infer $2.0 < pK_a < 3.5$ for the μ-hydroxo group of $[Fe_2(OH)(OAc)_2(TMIP)_2]^{3+}$. The analogous inference led to an estimated pK_a of 3.5 for the μ-hydroxo group of $[Fe_2(OH)(OAc)_2(HB(pz)_3)_2]^{+}$.[22]

With TMIP, only the aqueous method was successful for assembly and isolation of the μ-hydroxo complex. However, $[Fe_2(OH)(OAc)_2(TMIP)_2](ClO_4)_2BF_4$ was readily prepared in situ by addition of 1 equiv of HBF_4 to $[Fe_2O(OAc)_2(TMIP)_2](ClO_4)_2$ in acetonitrile. This method was also successful to a lesser extent for the analogous TIP-containing complex.

Assembly of $[Mn_2O(OAc)_2(TMIP)_2]X_2$ (X = PF_6 or ClO_4) used a method similar to that for assembly of $[Mn_2O(OAc)_2(HB(pz)_3)_2]$, which consists essentially of adding the tridentate capping ligand to a stirred suspension of manganese(III) acetate dihydrate plus the counteranion in acetonitrile.[5a] Strict exclusion of air was found to be critical at all stages of reaction and workup. Analytically pure material was obtained in lower yields (11% for the PF_6^- salt and 35% for the ClO_4^- salt) than for the analogous diiron(III) complexes. While we have yet to identify the contaminants, the relative difficulty in obtaining pure material may be due to the tendency of these types of dimanganese(III) complexes to disproportionate, especially in the presence of water.[5b,6] Once formed and isolated, however, $[Mn_2O(OAc)_2(TMIP)_2]^{2+}$ salts were found to be reasonably stable (i.e., for days to weeks) under anaerobic conditions either as a solid or as a solution in dry acetonitrile. Our attempts to prepare the corresponding dimanganese(III) complexes containing TIP in place of TMIP have been unsuccessful.

A possible reason for the greater difficulty in preparations of $[M_2O(O_2CR)_2L]^{2+}$ with L = TIP than with L = TMIP stems from the expected rotation of the imidazol-2-yl groups around their P–C bonds. Such rotation is expected to be sterically hindered by the *N*-methyl groups of TMIP such that all three N(3) atoms tend to point inward toward each other, thereby enhancing the tridentate chelating ability compared to that of TIP.

(22) Hartman, J. R.; Rardin, R. L.; Chaudhuri, P.; Pohl, K.; Wieghardt, K.; Nuber, B.; Weiss, J.; Papaefthymiou, G. C.; Frankel, R. B.; Lippard, S. J. *J. Am. Chem. Soc.* **1987**, *109*, 7387.

Table IV. Selected Interatomic Distances (Å) and Angles (deg) for $[M_2O(OAc)_2(TMIP)_2]^{2+}$ (M_2 = $Fe_2(\cdot 3CH_3CN\cdot(C_2H_5)_2O)$, $Mn_2(\cdot 2CH_3CN\cdot 0.5(C_2H_5)_2O)$)

	Fe	Mn		Fe	Mn
M(1)-M(2)	3.158 (2)	3.164 (5)	M(1)-N(11)	2.192 (6)	2.061 (14)
M(1)-O(1)	1.797 (4)	1.797 (11)	M(1)-N(31)	2.169 (5)	2.225 (15)
M(2)-O(1)	1.804 (5)	1.781 (11)	M(1)-N(51)	2.168 (6)	2.093 (15)
M(1)-O(4)	2.040 (5)	2.115 (13)	M(2)-N(12)	2.182 (6)	2.072 (14)
M(2)-O(3)	2.032 (5)	2.155 (13)	M(2)-N(32)	2.150 (6)	2.054 (15)
M(2)-O(5)	2.037 (5)	1.993 (13)	M(2)-N(52)	2.133 (6)	2.262 (15)
M(1)-O(2)	2.054 (5)	1.965 (13)			

	Fe	Mn		Fe	Mn
O(1)-M(1)-O(2)	96.1 (2)	95.9 (5)	O(1)-M(2)-O(3)	97.5 (2)	95.9 (5)
O(1)-M(1)-O(4)	96.5 (2)	93.9 (5)	O(1)-M(2)-O(5)	96.8 (2)	95.3 (5)
O(2)-M(1)-O(4)	92.9 (2)	94.8 (5)	O(3)-M(2)-O(5)	92.0 (2)	94.3 (5)
O(1)-M(1)-N(11)	176.7 (2)	176.4 (6)	O(1)-M(2)-N(12)	177.5 (2)	176.6 (6)
O(1)-M(1)-N(31)	95.0 (2)	96.4 (5)	O(1)-M(2)-N(32)	95.9 (2)	91.3 (6)
O(1)-M(1)-N(51)	99.2 (2)	90.2 (5)	O(1)-M(2)-N(52)	96.7 (2)	95.0 (5)
O(2)-M(1)-N(11)	81.5 (2)	87.7 (6)	O(3)-M(2)-N(12)	82.4 (2)	84.4 (6)
O(2)-M(1)-N(31)	92.2 (2)	90.2 (6)	O(3)-M(2)-N(32)	91.0 (2)	89.1 (5)
O(2)-M(1)-N(51)	164.4 (2)	173.0 (5)	O(3)-M(2)-N(52)	165.7 (2)	167.5 (5)
O(4)-M(1)-N(11)	86.0 (2)	85.6 (6)	O(5)-M(2)-N(12)	85.7 (2)	88.1 (6)
O(4)-M(1)-N(31)	166.9 (2)	168.0 (5)	O(5)-M(2)-N(32)	166.5 (2)	172.3 (6)
O(4)-M(1)-N(51)	88.1 (2)	88.2 (5)	O(5)-M(2)-N(52)	87.8 (2)	90.9 (5)
N(11)-M(1)-N(31)	82.8 (2)	83.7 (6)	N(12)-M(2)-N(32)	81.6 (2)	85.2 (6)
N(11)-M(1)-N(51)	83.1 (2)	86.2 (6)	N(12)-M(2)-N(52)	83.3 (2)	84.3 (6)
N(31)-M(1)-N(51)	83.8 (2)	85.8 (6)	N(32)-M(2)-N(52)	86.1 (2)	84.5 (6)
M(1)-O-M(2)	122.7 (2)	124.4 (6)			

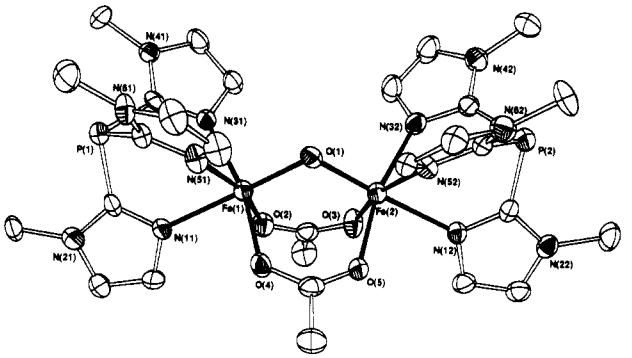

Figure 1. Structure of the diiron(III) complex in $[Fe_2O(OAc)_2(TMIP)_2](ClO_4)_2\cdot 3CH_3CN\cdot(C_2H_5)_2O$.

We have so far been unable to isolate dimetal(II) complexes containing manganese or iron with either TIP or TMIP either by reaction with divalent metal salts or by chemical reduction of $[Fe_2O(OAc)_2(TMIP)_2]^{2+}$. Such failures were not unexpected; in related systems, the bis(ligand) divalent metal complexes have greater thermodynamic stabilities. Only with MTACN, where steric hindrance by the methyl groups suppresses formation of the bis(ligand) complexes, have stable (μ-hydroxo)bis(μ-carboxylato)diiron(II) and -dimanganese(II) complexes been isolated.[5b,23]

Structures of the Iron Complexes. The previously reported ^1H NMR of $[Fe(TIP)_2](ClO_4)_3$ and $[Fe(TMIP)_2](ClO_4)_3$[9] show that these complexes are low-spin ferric and have D_{3d} symmetry in solution with the phosphorus atoms of the two ligands and the central iron atom lying along the 3-fold rotational axis. On the basis of the strong similarities in ^1H NMR spectra, the structures of $[Fe(TIP)_2](ClO_4)_3$ and $[Fe(TMIP)_2](ClO_4)_3$ are likely to be very similar to that of $[Fe(TICOH)_2]^{3+}$.[9,24]

The structure of the diiron complex in $[Fe_2O(OAc)_2(TMIP)_2](ClO_4)_2\cdot 3CH_3CN\cdot(C_2H_5)_2O$ is shown in Figure 1. Selected distances and angles are listed in Table IV. The structure of the (μ-oxo)bis(μ-carboxylato)diiron(III) core is typical of such complexes[3] with an average $Fe-O_{oxo}$ bond distance of 1.800 (5) Å, $Fe-O_{oxo}-Fe$ angle of 122.7 (2)°, and intramolecular Fe---Fe distance of 3.158 (2) Å. The two $Fe-N_{Im}$ bond distances trans to the oxo bridge are an average of 0.03 Å longer the four cis $Fe-N_{Im}$ bond distances, reflecting the trans influence of the oxo bridge. This structural trans effect appears to be somewhat smaller than that for (μ-oxo)bis(μ-carboxylato)diiron(III) complexes with the capping tridentate nitrogen ligands, TACN,[26] MTACN,[22] and $HB(pz)_3$,[26] where the trans Fe–N bond lengthening is in the range of 0.04-0.07 Å. While the trigonal contraction and uniformity that TMIP imposes on the coordination sphere would tend to minimize differences in cis vs trans Fe–N bond lengths, the distortions from idealized octahedral coordination spheres and deviations from linearity in the $N_{trans}-Fe-O_{oxo}$ angles in $[Fe_2O(OAc)_2(TMIP)_2](ClO_4)_2\cdot 3CH_3CN\cdot(C_2H_5)_2O$ are not significantly different from those in $[Fe_2O(OAc)_2(HB(pz)_3)_2]$.[26]

A ligand related to TMIP, namely TICOMe, has the three imidazolyl groups attached to a central carbon rather than phosphorus. Beer et al.[27] have recently shown that only two of the three imidazolyl groups of TICOMe coordinate to iron in the (μ-oxo)bis(μ-carboxylato)diiron(III) core of $[Fe_2O(MPDP)(TICOMe)_2Cl_2]$. A possible reason for the bidentate coordination is strain induced in TICOMe upon tridentate coordination through the imidazolyl nitrogens. The larger central phosphorus atom of TMIP may relieve this strain. A similar explanation was invoked

Table V. UV-Vis Absorption in the 300–400-nm Region, ^{57}Fe Mössbauer Data, and Magnetic Susceptibility for $[Fe_2O(O_2CR)_2(TMIP)_2]^{2+}$, $[Fe_2(OH)(O_2CR)_2(TMIP)_2]^{3+}$, and Oxyhemerythrin[a]

	λ, nm (ϵ_{2Fe}, M^{-1} cm^{-1})	δ_{Fe} (ΔE_Q), mm/s[b]	$-J$, cm^{-1}
$[Fe_2O(O_2CR)_2(TMIP)_2]^{2+}$	338 (7900)[c] 360 sh (6900)[c]	0.52 (1.61)[d]	120[d]
$[Fe_2(OH)(O_2CR)_2(TMIP)_2]^{3+}$	~370 sh (2200)[c]	0.46 (0.51)[d]	~17[c,d]
oxyhemerythrin	330 (6800)[e] 360 sh (5450)	0.54 (1.92)[f] 0.51 (1.09)	≥77[g]

[a] From this work unless noted otherwise. [b] At 4.2 K. [c] For O_2CR = OAc. [d] For O_2CR = OPr. [e] From ref 46. [f] From ref 47. [g] From refs 42 and 48.

(23) Chaudhuri, P.; Wieghardt, K.; Nuber, B.; Weiss, J. *Angew. Chem., Int. Ed. Engl.* **1985**, *24*, 778.
(24) Gorun, S. M., Ph.D. Thesis 1986, Massachusetts Institute of Technology, Cambridge, MA.
(25) Spool, A.; Williams, I. D.; Lippard, S. J. *Inorg. Chem.* **1985**, *24*, 2156.
(26) Armstrong, W. H.; Spool, A.; Papaefthymiou, G. C.; Frankel, R. B.; Lippard, S. J. *J. Am. Chem. Soc.* **1984**, *106*, 3653.
(27) Beer, R. H.; Tolman, W. B.; Bott, S. G.; Lippard, S. J. *Inorg. Chem.* **1989**, *28*, 4557.

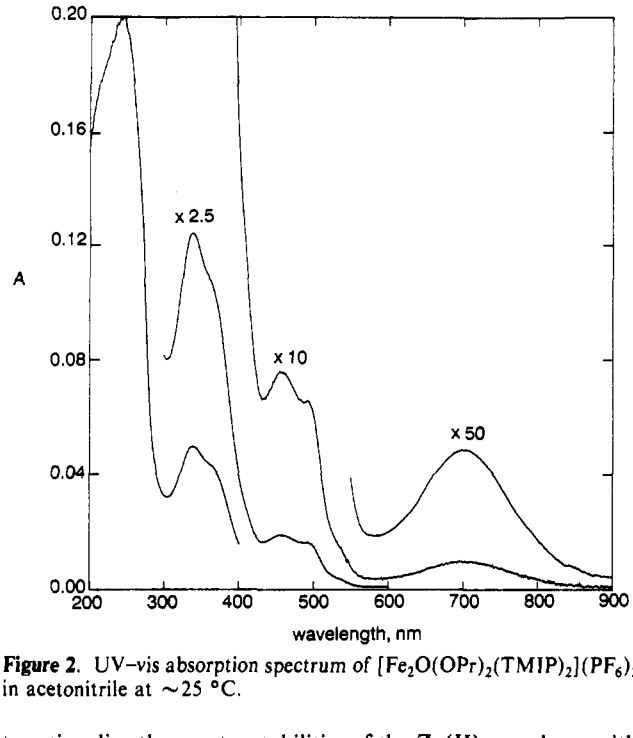

Figure 2. UV–vis absorption spectrum of $[Fe_2O(OPr)_2(TMIP)_2](PF_6)_2$ in acetonitrile at ~25 °C.

to rationalize the greater stabilities of the Zn(II) complexes with TIP compared to that with TICOH.[14b]

The hydroxo-bridged complex $[Fe_2(OH)(OAc)_2(TMIP)_2]^{3+}$ is essentially isostructural with its oxo-bridged counterpart. This statement is based on its spectroscopic and magnetic properties, which are discussed in the following section.

Spectroscopy and Magnetic Behavior of the Diiron(III) Complexes. Previously unreported data for these complexes are listed in Table V. ^1H NMR data for these complexes have been previously reported and analyzed,[9], as have resonance Raman data for $[Fe_2O(OPr)_2(TMIP)_2](PF_6)_2$.[13] This compound shows ν_s(Fe–O–Fe) (533 cm^{-1}) and ν_{as}(Fe–O–Fe) (749 cm^{-1}) frequencies typical of the (μ-oxo)bis(μ-carboxylato)diiron(III) core.[3] The symmetric stretching frequency and its ^{18}O isotope dependence correlate nicely with the $Fe–O_{oxo}–Fe$ bond angle of 122.7° observed in $[Fe_2O(OAc)_2(TMIP)_2](ClO_4)_2·3CH_3CN·(C_2H_5)_2O$.[13,28] Also typical of these complexes, the symmetric stretch appears to be in resonance with an electronic transition near 400 nm, which does not correspond to a prominent feature in the absorption spectrum (cf. Figure 2).[13] The UV–vis absorption spectrum of $[Fe_2O(OPr)_2(TMIP)_2](PF_6)_2$ in acetonitrile shown in Figure 2 closely resembles those of $[Fe_2O(OAc)_2(TIP)_2](ClO_4)_2·H_2O$ and $[Fe_2O(OAc)_2(TMIP)_2](ClO_4)_2·CH_3CN$ in the same solvent. These spectra are very similar to those reported for (μ-oxo)bis(μ-carboxylato)diiron(III) complexes with other capping ligands.[3] The prominent absorption bands at ~340 and 360 nm (ϵ_{2Fe} = 6000–8000 M^{-1} cm^{-1}) have most recently been assigned to oxo → iron charge-transfer transitions.[29]

Despite the relatively small differences between cis and trans Fe–N bond distances seen in $[Fe_2O(OAc)_2(TMIP)_2](ClO_4)_2·3CH_3CN·(C_2H_5)_2O$, the previously reported ^1H NMR spectra of $[Fe_2O(OAc)_2(TIP)_2]^{2+}$ and $[Fe_2O(OAc)_2(TMIP)_2]^{2+}$ appear to be highly sensitive to the structural trans effect of the oxo bridge.[9] Pairs of resonances in a 2:1 intensity ratio for each position on the imidazolyl ring are observed. Within each pair, the cis (i.e., the more intense) imidazolyl resonance appears from 0.5 to 4 ppm farther downfield; the shorter cis than trans $Fe–N_{Im}$ bonds (Table I) apparently allow more unpaired electron spin density to be delocalized onto the cis imidazolyl rings. It is noteworthy that a trans effect of the hydroxo bridge, although reduced compared to that in the corresponding oxo-bridged complex, is still evident in the pair of N-CH_3 resonances at ~16 and 17 ppm in ^1H NMR spectrum of $[Fe_2(OH)(OAc)_2(TMIP)_2]^{3+}$.[9] No lengthening of the trans Fe–N bond was noted in the crystal structure of the analogous (μ-hydroxo)bis(μ-carboxylato)diiron(III) complex $[Fe_2(OH)(OAc)_2(HB(pz)_3)_2]^+$.[30] Nevertheless, we conclude that in these diiron(III) complexes the amount of spin delocalized into the σ-bond system of the imidazolyl rings and, hence, the isotropic shifts of the imidazolyl ring protons and methyls are exquisitely sensitive to $Fe–N_{Im}$ bond distances. Some alternative explanations for the NMR sensitivity can be ruled out. No significant dipolar contributions to these shifts are expected for the spherically symmetric d-electron distribution of high-spin Fe(III), and the value of $-J$ for the hydroxo-bridged complex (vide infra) means that the various spin levels are populated nearly uniformly at room temperature.

Variable temperature magnetic susceptibility measurements on $[Fe_2O(OPr)_2(TMIP)_2](PF_6)_2·CH_3CN$ using SQUID susceptometry between 10 and 300 K were fit to a standard equation for temperature-dependent susceptibility derived from the general isotropic spin exchange Hamiltonian $\hat{H}_{ex} = -2J\hat{S}_1·\hat{S}_2$ with $S_1 = S_2 = {}^5/_2$ and $J < 0$, indicating antiferromagnetism.[31] g and J were allowed to vary, and a diamagnetic correction was applied. The best fit gave g = 1.99 (2) and $-J$ = 120 (2) cm^{-1}. This value of $-J$ is within the range previously reported for the (μ-oxo)bis(μ-carboxylato)diiron(III) core (109–132 cm^{-1}).[3] An Evans susceptibility measurement at ~23 °C on $[Fe_2O(OAc)_2(TMIP)_2](ClO_4)_2·CH_3CN$ in acetonitrile gave an effective magnetic moment of 1.66 μ_B/Fe, which is also typical for this tribridged core when $-J$ ~ 120 cm^{-1} [3] and which confirms the integrity of the core in solution.

Only one example of a complex containing the (μ-hydroxo)bis(μ-carboxylato)diiron(III) core has been previously reported, namely, $[Fe_2(OH)(OAc)_2(HB(pz)_3)_2](ClO_4)·0.5CH_2Cl_2$.[30] Additional examples are desirable in order to identify characteristic spectroscopic and magnetic features of this core. The integrity of the (μ-hydroxo)bis(μ-carboxylato)diiron(III) core of $[Fe_2(OH)(OPr)_3(TMIP)_2](ClO_4)_3·CH_3CN·H_2O$ in solution was confirmed by an Evans measurement in acetonitrile, which gave a room-temperature effective magnetic moment of 4.31 μ_B/Fe. This value is very similar to the room-temperature effective magnetic moment of 4.36 μ_B/Fe determined for solid $[Fe_2(OH)(OAc)_2(HB(pz)_3)_2](ClO_4)·0.5CH_2Cl_2$, whose X-ray crystal structure exhibits the (μ-hydroxo)bis(μ-carboxylato)diiron(III) core.[30] In addition, the chemical shift of the room-temperature ^1H NMR resonance of the bridging acetate methyl in $[Fe_2(OH)(OAc)_2(TMIP)_2](ClO_4)_2BF_4$ (66 ppm[9]) is very similar to that of the bridging acetate methyl in $[Fe_2(OH)(OAc)_2(HB(pz)_3)_2](ClO_4)·0.5CH_2Cl_2$ (68.7 ppm).[30] The isotropic shift of the bridging acetate methyl resonance in tribridged diiron(III) complexes shows a close correlation with the extent of antiferromagnetic coupling.[9,32] $-J$ = 17 cm^{-1} was reported for $[Fe_2(OH)(OAc)_2(HB(pz)_3)_2](ClO_4)·0.5CH_2Cl_2$,[30] and comparisons with our NMR[9] and magnetic measurements in acetonitrile solution imply a very similar (but perhaps slightly larger) value of $-J$ for both $[Fe_2(OH)(OAc)_2(TMIP)_2]^{3+}$ and $[Fe_2(OH)(OPr)_2(TMIP)_2]^{3+}$. These additional examples indicate that $-J$ ~ 17 cm^{-1} is characteristic of the (μ-hydroxo)bis(μ-carboxylato)diiron(III) core.

The visible absorption spectrum of $[Fe_2(OH)(OAc)_2(TMIP)_2](ClO_4)_2BF_4$ shows only a weak peak at 455 nm (ϵ_{2Fe} = 450 M^{-1} cm^{-1}), and a shoulder at ~370 nm (ϵ_{2Fe} = 2200 M^{-1} cm^{-1}) superimposed on a steeply rising absorbance into the UV. This spectrum differs from that reported for $[Fe_2(OH)(OAc)_2(HB(pz)_3)_2](ClO_4)·0.5CH_2Cl_2$.[30] Therefore, no characteristic absorption spectrum for the (μ-hydroxo)bis(μ-carboxylato)di-

(28) Turowski, P. N.; Armstrong, W. H.; Roth, M. E.; Lippard, S. J. *J. Am. Chem. Soc.* **1990**, *112*, 681.
(29) Reem, R. C.; McCormick, J. M.; Richardson, D. E.; Devlin, F. J.; Stephens, P. J.; Musselman, R. L.; Solomon, E. I. *J. Am. Chem. Soc.* **1989**, *111*, 4688.
(30) Armstrong, W. H.; Lippard, S. J. *J. Am. Chem. Soc.* **1984**, *106*, 4632.
(31) O'Connor, C. J. *Prog. Inorg. Chem.* **1982**, *29*, 204.
(32) Arafa, I. M.; Goff, H. M.; Davis, S. S.; Murch, B. P.; Que, L., Jr. *Inorg. Chem.* **1987**, *26*, 2779.

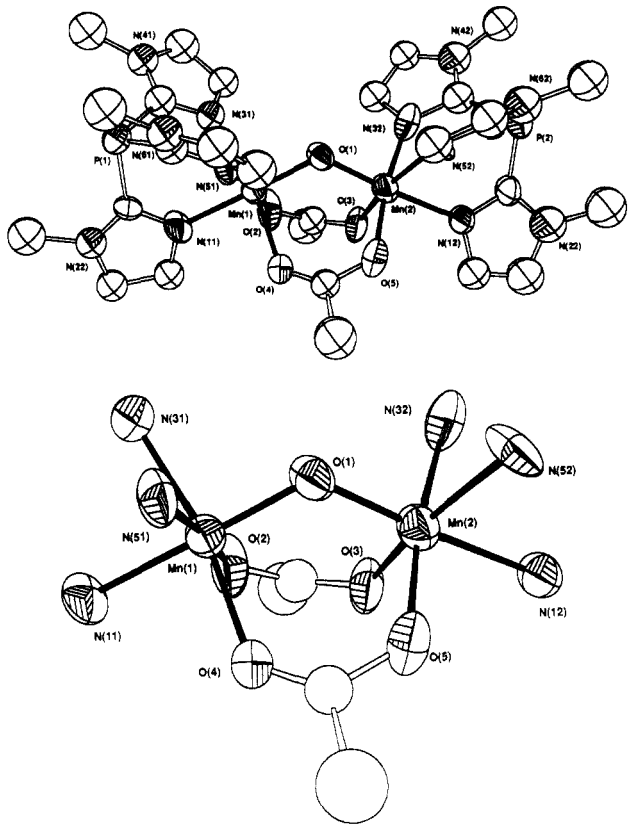

Figure 3. Top: (A) structure of the dimanganese(III) complex in $[Mn_2O(OAc)_2(TMIP)_2](ClO_4)_2 \cdot 2CH_3CN \cdot 0.5(C_2H_5)_2O$. Bottom: (B) same structure as in part A except that only core and terminally coordinating nitrogen atoms are shown for clarity.

iron(III) core can yet be identified. With TMIP as capping ligand the absorption spectrum of the hydroxo-bridged complex is clearly different from that of the oxo-bridged complex, especially in the region of 300–400 nm.[33]

^{57}Fe Mössbauer spectra obtained at 4.2 K gave the following values for isomer shift (quadrupole splitting), δ_{Fe} (ΔE_Q), in mm/s: for $[Fe_2O(OPr)_2(TMIP)_2](PF_6)_2 \cdot CH_3CN$, 0.52 (1.61); for $[Fe_2O(OAc)_2(TMIP)_2](ClO_4)_2 \cdot CH_3CN$, 0.52 (1.65); for $[Fe_2(OH)(OPr)_2(TMIP)_2](ClO_4)_3 \cdot CH_3CN \cdot H_2O$, 0.46 (0.51). The former two sets of values are within the ranges previously reported for the (μ-oxo)bis(μ-carboxylato)diiron(III) core (0.37–0.56 (1.27–1.80)).[3] The values for the hydroxo-bridged complex are similar to those of $[Fe_2(OH)(OAc)_2(HB(pz)_3)_2](ClO_4) \cdot 0.5CH_2Cl_2$ (0.47 (0.25)).[22] The two sets of examples now available indicate that conversion of the (μ-oxo)- to the (μ-hydroxo)bis(μ-carboxylato)diiron(III) core results in a dramatic reduction in quadrupole splitting. While many factors can contribute to the more spherically symmetric electric field gradient implied by the reduced quadrupole splitting, the most obvious structural change with which to associate this reduction is lengthening of the Fe–O_{oxo} bond upon protonation of the oxo bridge and concomitant shortening of the trans Fe–N bond.

Structure of $[Mn_2O(OAc)_2(TMIP)_2](ClO_4)_2 \cdot 2CH_3CN \cdot 0.5(C_2H_5)_2O$. The structure of the dimanganese(III) complex is shown in Figure 3. Selected interatomic distances and angles of this complex are compared to those of the diiron(III) congener in Table IV. This comparison illustrates the close similarity in the structures of these (μ-oxo)diiron(III) and -dimanganese(III) cores, including the M(1)–M(2) and M–O_{oxo} distances and M(1)–O–M(2) angles. The most notable differences in the dimanganese(III) complex are the absence of lengthened Fe–N_{Im} bonds trans to the oxo bridge and a significant distortion in both the Mn(1) and Mn(2) coordination spheres. This distortion can be described as a lengthening of one set of *trans*-N–Mn–O_{OAc} bonds. In the structure shown in Figure 3B, these elongated bonds are N(31)–Mn(1)–O(4) and N(52)–Mn(2)–O(3). These two sets of trans N–Mn–O_{OAc} atoms also show a greater deviation from linearity than do the other sets. The N–Mn–O_{OAc} bond lengthening is presumably due to the Jahn–Teller effect expected for Mn(III) in the high-spin d^4 configuration, but the distortion is distinct from that observed in the other structurally characterized complexes that contain (μ-oxo)bis(μ-carboxylato)dimanganese(III) cores capped by tridentate ligands, namely, $[Mn_2O(OAc)_2(HB(pz)_3)_2]$,[5a] $[Mn_2O(OAc)_2(TACN)_2]^{2+}$, and $[Mn_2O(OAc)_2(MTACN)_2]^{2+}$.[5b,c] In these latter complexes, the most pronounced distortion in each Mn coordination sphere is a *shortening* of the Mn–N bond that is trans to the Mn–O_{oxo} bond. Nevertheless, when coupled with the short Mn–O_{oxo} bond distances, the major electronic consequence is expected to be the same for these two types of distortions. That is, the d orbital directed along the Mn–O_{oxo} bond axis, usually labeled d_{z^2},[5] should be unoccupied. The two distinct types of distortion described above indicate a flexibility in the Mn(III) coordination sphere in these complexes. In fact the type of static distortion in the Mn coordination sphere described above for $[Mn_2O(OAc)_2(TMIP)_2](ClO_4)_2 \cdot 2CH_3CN \cdot 0.5(C_2H_5)_2O$ does not persist in solution (vide infra).[34]

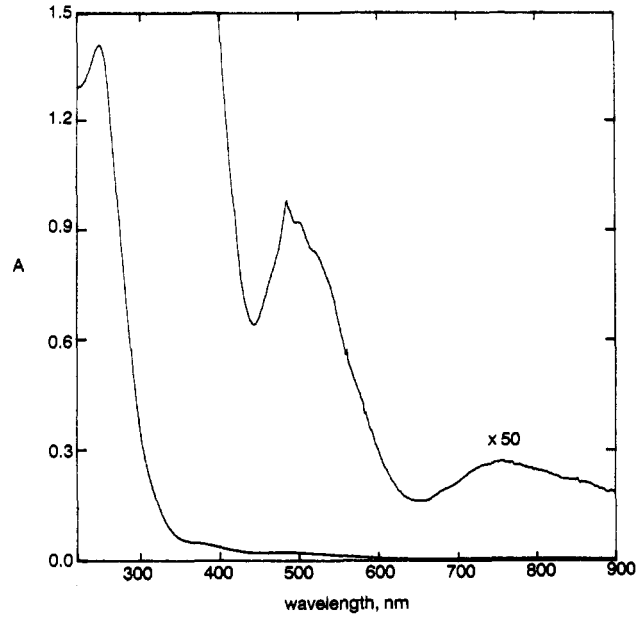

Figure 4. UV–vis absorption spectrum of $[Mn_2(OAc)_2(TMIP)_2](PF_6)_2$ in acetonitrile at ~25 °C.

Electrochemistry of the Dimanganese(III) Complex. Cyclic voltammetry at a Pt-disk electrode on $[Mn_2O(OAc)_2(TMIP)_2](ClO_4)_2$ in acetonitrile under anaerobic conditions showed a quasi-reversible one-electron wave at $E_{1/2}$ = 0.59 V vs ferrocenium/ferrocene and an irreversible wave at –0.70 V vs ferrocenium/ferrocene. The isostructural complex $[Mn_2O(OAc)_2(MTACN)_2](ClO_4)_2 \cdot H_2O$ exhibits two very similar waves, which were attributed to the $Mn^{III}Mn^{IV}/Mn^{III}Mn^{III}$ redox couple and $Mn^{III}Mn^{III} \rightarrow Mn^{III}Mn^{II}$ reduction, respectively.[5b] When the potentially oxidizable TMIP was subjected to cyclic voltammetry under the same conditions, no waves were observed between +2.0 and –1.0 V vs Ag/AgCl.

Spectroscopy and Magnetic Behavior of the Dimanganese(III) Complex. The UV–vis absorption spectrum of $[Mn_2O(OAc)_2$-

(33) The absorption spectra of $[Fe_2(OH)(OAc)_2(TMIP)_2](ClO_4)_2BF_4$ were obtained in CD_3CN, and ^1H NMR spectra of these same solutions showed little or no contamination by either $[Fe_2O(OAc)_2(TMIP)_2](ClO_4)_2$ or $[Fe(TMIP)_2](ClO_4)_2$. These ^1H NMR spectra also ruled out significant contamination by any trinuclear "basic iron acetate" complexes, which have a prominent acetate methyl resonance at ~31 ppm.[9]

(34) However, the same type and extent of distortion in the Mn coordination sphere occurs in both the monoclinic and orthorhombic forms of $[Mn_2O(OAc)_2(TMIP)_2](ClO_4)_2 \cdot 2CH_3CN \cdot 0.5(C_2H_5)_2O$, arguing against crystal packing as the driving force for this type of distortion.

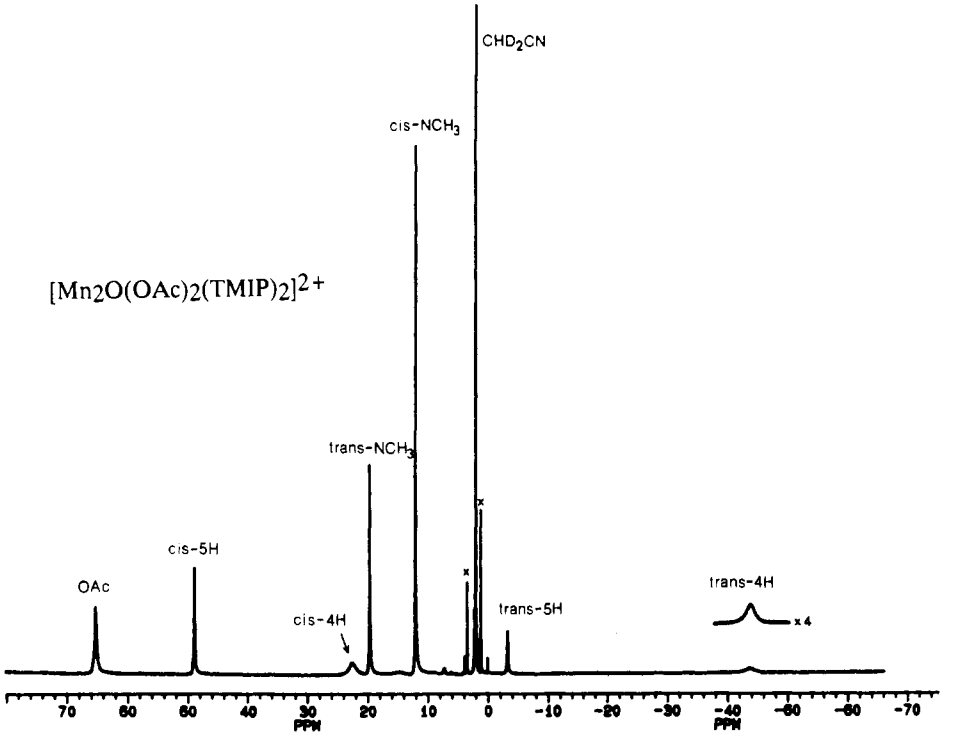

Figure 5. ^{1}H NMR spectrum of $[Mn_2O(OAc)_2(TMIP)_2](PF_6)_2$ in CD_3CN at ~23 °C. × = impurity. Proposed assignments are given above each resonance.

$(TMIP)_2](PF_6)_2$ shown in Figure 4 is nearly identical with that of the perchlorate salt and closely resembles those previously reported for $[Mn_2O(OAc)_2(HB(pz)_3)_2]$[5a] and $[Mn_2O(OAc)_2(MTACN)_2](ClO_4)_2$.[5b] This similarity indicates that the spectrum in Figure 4 is characteristic of the (μ-oxo)bis(μ-carboxylato)dimanganese(III) core.[6] The room-temperature effective magnetic moment of $[Mn_2O(OAc)_2(TMIP)_2](PF_6)_2$ in acetonitrile was found to be 5.01 μ_B/Mn, which is between the values of 4.92 μ_B/Mn and 5.12 μ_B/Mn found for $[Mn_2O(OAc)_2(HB(pz)_3)_2]$,[5a] and $[Mn_2O(OAc)_2(MTACN)_2](ClO_4)_2$,[5b] respectively. The chemical shifts of the bridging acetate methyl resonances in ^{1}H NMR spectra of $[Mn_2O(OAc)_2(TMIP)_2]^{2+}$ and $[Mn_2O(OAc)_2(HB(pz)_3)_2]$[5a] are both at 66 ppm, consistent with their very similar room-temperature magnetic moments. Data obtained from variable-temperature magnetic susceptibility measurements using SQUID susceptometry between 10 and 300 K on both solid salts of $[Mn_2O(OAc)_2(TMIP)_2]^{2+}$ were fit to the Hamiltonian described above for $S_1 = S_2 = 2$. These fits indicated a very small antiferromagnetic exchange coupling with $-J \leq 0.5$ cm^{-1} for the $(PF_6)_2$ salt and $-J \leq 0.2$ cm^{-1} for the $(ClO_4)_2 \cdot 2CH_3CN$ salt. These values are within the range found previously for other (μ-oxo)bis(μ-carboxylato)dimanganese(III) complexes (-3.4 cm$^{-1} \leq J \leq 9$ cm^{-1}).[5a,b,35] The magnetic data for both salts of $[Mn_2O(OAc)_2(TMIP)_2]^{2+}$ are incompatible with ferromagnetic coupling. A zero-field splitting term was not included in the fits because we have no independent measure of its magnitude and because its inclusion would not change the most important result, namely, that $[Mn_2O(OAc)_2(TMIP)_2]^{2+}$ shows extremely weak antiferromagnetism.

The much lower values of $-J$ for the dimanganese(III) complex than for the isostructural diiron(III) complex (120 cm^{-1}) together with the empty d_{z^2} orbitals along the $Mn-O_{oxo}$ bond axis inferred from the crystal structure reinforces the idea that the d_{z^2} orbitals are involved in a major pathway for magnetic coupling in the (μ-oxo)bis(μ-carboxylato)dimetal(III) complexes.[5a] Bossek et al.[36] have recently provided an elegant demonstration that orbital occupancy in the d_{z^2}–d_{xz} "crossed" pathway determines both the sign and magnitude of spin coupling in such complexes. In the case of the (μ-oxo)bis(μ-carboxylato)dimanganese(III) core, the coupling is apparently inherently weak because two d_{z^2}–d_{xz} ferromagnetic pathways oppose the d_{yz}–d_{yz} antiferromagnetic pathway.[37] Thus, a delicate balance of structural and electronic factors can determine the sign of J. Including $[Mn_2O(OAc)_2(TMIP)_2]^{2+}$, seven structurally and magnetically characterized examples of this core are presently available, four of which are either weakly antiferromagnetic or uncoupled and three of which are weakly ferromagnetic.[5,6,35,38] No obvious structural features that can be associated with the sign of J have emerged. The magnetic behavior of $[Mn_2O(OAc)_2(TMIP)_2]^{2+}$ most closely resembles that of $[Mn_2O(OAc)_2(HB(pz)_3)_2]$ ($J \sim -0.5$ cm^{-1}[5a]) even though these two complexes have different types of distortions in the manganese coordination sphere, as discussed above.

The ^{1}H NMR spectrum of $[Mn_2O(OAc)_2(TMIP)_2](PF_6)_2$ is shown in Figure 5 with proposed assignments given above each isotropically shifted resonance. The perchlorate salt gives an identical spectrum. The assignments are based on relative intensities and on analogy to those of $[Mn_2O(OAc)_2(HB(pz)_3)_2]$.[5a] The empty d_{z^2} orbitals referred to above mean that, for the imidazolyl rings trans to the oxo bridge in $[Mn_2O(OAc)_2(TMIP)_2]^{2+}$, delocalization of unpaired electron spin can occur only through the π system, whereas spin delocalization through both σ and π systems is available to the cis imidazolyl rings. Delocalization of unpaired spin through the π system of imidazole is known to result in upfield ^{1}H NMR isotropic shifts for all ring protons and downfield isotropic shifts for ring methyls, whereas delocalization of unpaired spin through the σ system of imidazole results in downfield isotropic shifts for both ring protons and ring methyls.[9,39] The isotropically shifted resonances in Figure 5 have been assigned accordingly. The intensities of resonances assigned to the trans imidazolyl ring protons and *N*-methyl are half those of their cis counterparts, which is consistent with the ratio of trans to cis imidazolyl rings in $[Mn_2O(OAc)_2(TMIP)_2]^{2+}$. In contrast to the

(35) Ménage, S.; Girerd, J. J.; Gleizes, A. *J. Chem. Soc., Chem. Commun.* **1988**, 431.
(36) Bossek, U.; Weyhermüller, T.; Wieghardt, K.; Bonvoisin, J.; Girerd, J. J. *J. Chem. Soc., Chem. Commun.* **1989**, 633.
(37) We thank Karl Wieghardt for a helpful discussion on this point.
(38) Vincent, J. B.; Folting, K.; Huffman, J. C.; Christou, G. *Biochem. Soc. Trans.* **1988**, *16*, 822–823.
(39) (a) Satterlee, J. D.; La Mar, G. N. *J. Am. Chem. Soc.* **1976**, *98*, 2804. (b) Goff, H. M.; La Mar, G. N. *J. Am. Chem. Soc.* **1977**, *99*, 6599.

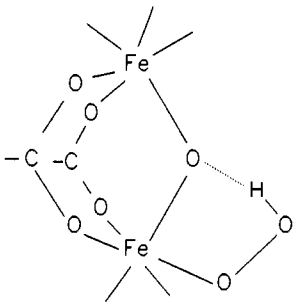

oxyhemerythrin

Figure 6. Proposed structure for the active site of oxyhemerythrin. Adapted from ref 43.

crystal structure, the ^{1}H NMR data indicate that the average chemical and magnetic environments of the two cis imidazolyl rings coordinated to each Mn atom are identical in solution on the NMR time scale.

The preceding analysis assumes that the isotropic shifts are predominantly contact in origin. Consistent with this assumption, we find that the isotropic shifts of all of the assigned resonances depicted in Figure 5 show Curie law behavior with no significant deviations from linearity in the reciprocal temperature plots of shifts at eight temperatures in the range 233–303 K. In contrast to the behavior of the corresponding diiron(III) complexes, the resonances of the 4-H protons, i.e., those closest to the metal atoms, are observable in the spectrum of Figure 5, indicating a shorter T_{1e} for the dimanganese(III) than the diiron(III) complex.

Conclusions and Some Implications for Dimetal(III) Sites in Proteins. TMIP can be added to the list of capping ligands that stabilize (μ-oxo/hydroxo)bis(μ-carboxylato)diiron(III) and dimanganese(III) cores. TIP appears to be less versatile in this regard; under essentially the same conditions as used for TMIP, TIP forms a stable complex only with the (μ-oxo)bis(μ-carboxylato)diiron(III) core. The results presented here show that terminal imidazolyl ligands, when compared with other terminal ligands, do not drastically alter the structural, spectroscopic, and magnetic properties of (μ-oxo)bis(μ-carboxylato)diiron(III)[3] and dimanganese(III) cores.[5,6] With the possible exception of the absorption spectrum, the analogous statement applies to the (μ-hydroxo)bis(μ-carboxylato)diiron(III) core. $[Fe_2O(OAc)_2(TMIP)_2]^{2+}$ provides a synthetic analogue for the diiron(III) site in methemerythrin that differs only by the absence of one imidazolyl ligand in the protein. The trans influence of the oxo bridge in $[Fe_2O(OAc)_2(TMIP)_2](ClO_4)_2\cdot 3CH_3CN\cdot(C_2H_5)_2O$ results in an average 0.03 Å lengthening of the trans vs cis Fe–N_{Im} bonds. The constraints toward uniformity imposed by TMIP on coordination of its three imidazolyl groups are unlikely to be present in a protein. The absence of such constraints could be the reason that, in azidometmyohemerythrin, all three cis Fe–N_{Im} bond distances are more than 0.1 Å shorter than the two trans Fe–N_{Im} distances (cf. Chart I).[40]

Hemerythrin has never been shown to contain a hydroxo-bridged diiron(III) site; its existence in the protein may be precluded by the inherently low pK_a of the hydroxo bridge (≤3.5), as inferred from aqueous assemblies of $[Fe_2(OH)(OAc)_2(TMIP)_2]^{3+}$ and $[Fe_2(OH)(OAc)_2(HB(pz)_3)_2]^{+}$.[22] However, there are few spectroscopic signatures for this hydroxo-bridged site. The two sets of oxo- and hydroxo-bridged complexes for which data are now available suggest that one such signature is an ^{57}Fe Mössbauer doublet with a similar isomer shift but much smaller quadrupole splitting than for the oxo-bridged sites (cf. Table V and ref 22). There are, as yet, no authenticated examples of a non-sulfur diiron(III) site in a protein with quadrupole splittings significantly less than 1 mm/s.[4] However, a relevant observation is that the quadrupole splitting of 1.57 mm/s for methemerythrin is reduced to 0.99 mm/s for (μ-sulfido)methemerythrin.[41] In the latter derivative, the oxo bridge is replaced by a sulfido bridge, which, like a hydroxo bridge, is expected to have a relatively smaller trans influence than an oxo bridge, thereby resulting in a more uniform set of Fe–N_{Im} distances and a smaller electric field gradient at iron. A more uniform set of Fe–N_{Im} distances in (μ-sulfido)methemerythrin is indeed indicated by the smaller range of isotropically shifted imidazolyl N–H resonances in ^{1}H NMR spectra of (μ-sulfido)methemerythrin compared to that for methemerythrin.[42]

The structure proposed for the diiron site in oxyhemerythrin is shown in Figure 6[43] and consists of a hydroperoxo ligand that forms a hydrogen bond to the oxo bridge of a (μ-oxo)bis(μ-carboxylato)diiron(III) core. The previous comparisons[9] of the ^{1}H NMR spectra of $[Fe_2O(OAc)_2(TIP)_2]^{2+}$ and $[Fe_2(OH)(O_2CR)_2(TMIP)_2]^{3+}$ to that of oxyhemerythrin[42] support the placement of the proton in Figure 6 predominantly on the peroxo ligand rather than the oxo bridge. The comparisons in Table V of the UV–vis absorption in the "oxo-dimer" region (300–400 nm),[29] ^{57}Fe Mössbauer spectra, and $-J$ values of $[Fe_2O(O_2CR)_2(TMIP)_2]^{2+}$ and $[Fe_2(OH)(O_2CR)_2(TMIP)_2]^{3+}$ to those of oxyhemerythrin also support the location of the proton in Figure 6.

It is likely that some dimanganese(III) sites in proteins contain an oxo bridge and terminal imidazolyl ligands,[6] and $[Mn_2O(OAc)_2(TMIP)_2]^{2+}$ has these features. As has been noted for the other complexes containing the (μ-oxo)bis(μ-carboxylato)dimanganese(III) core,[5,6] the absorption spectrum of $[Mn_2O(OAc)_2(TMIP)_2]^{2+}$ strrongly resembles those of proteins that contain dimanganese(III) sites, especially in the 400–600-nm region.[6-8] The absorption bands in this region apparently arise predominantly from d–d and charge-transfer transitions within the (μ-oxo)bis(μ-carboxylato)dimanganese(III) core.[5a,6] However, in the absence of more detailed spectral analysis and further synthetic modeling, we would caution against using this region of the absorption spectrum alone to either diagnose the core structure or to rule out the presence of a mononuclear manganese(III) site with similar ligands, such as that in manganese(III)–superoxide dismutase.[44,45] The results reported here indicate that ^{1}H NMR could be a useful structural and magnetic probe of (μ-oxo)dimanganese(III) sites in proteins. For example, placement of imidazolyl rings cis or trans to the oxo bridge should be readily determinable. The isotropically shifted N–H resonances of the imidazolyl ligands to the (μ-oxo)bis(μ-carboxylato)diiron(III) core in oxy- and methemerythrin have been identified as broad, solvent-exchangeable features in ^{1}H NMR spectra.[42] The shorter T_{1e} of the (μ-oxo)bis(μ-carboxylato)dimanganese(III) core could facilitate observation of ligand ^{1}H NMR resonances in proteins containing this latter core.

Acknowledgment. This research was supported by NIH Grants GM37851 and GM40388 (D.M.K.) and GM16406 (P.G.D.). D.M.K. is an NIH Research Career Development Awardee during 1988–1993. We thank Mr. Ji-Hu Zhang for experimental assistance in the initial stages of this work.

(40) Sheriff, S.; Hendrickson, W. A.; Smith, J. L. *J. Mol. Biol.* **1987**, *197*, 273–296.

(41) Lukat, G. S.; Kurtz, D. M., Jr.; Shiemke, A. K.; Loehr, T. M.; Sanders-Loehr, J. *Biochemistry* **1984**, *23*, 6416.

(42) (a) Maroney, M. J.; Kurtz, D. M., Jr.; Nocek, J. M.; Pearce, L. L.; Que, L., Jr. *J. Am. Chem. Soc.* **1986**, *108*, 6871. (b) Maroney, M. J.; Lauffer, R. B.; Que, L., Jr.; Kurtz, D. M., Jr. *J. Am. Chem. Soc.* **1984**, *106*, 6445.

(43) Stenkamp, R. E.; Sieker, L. C.; Jensen, L. H.; McCallum, J. D.; Sanders-Loehr, J. *Proc. Natl. Acad. Sci. U.S.A.* **1985**, *82*, 713.

(44) (a) Keele, B. B., Jr.; McCord, J. M.; Fridovich, I. *J. Biol. Chem.* **1970**, *245*, 6176. (b) Fee, J. A.; Shapiro, E. R.; Moss, T. H. *J. Biol. Chem.* **1976**, *251*, 6157.

(45) Stallings, W. C.; Pattridge, K. A.; Strong, R. K.; Ludwig, M. L. *J. Biol. Chem.* **1985**, *260*, 16424.

(46) Garbett, K.; Darnall, D. W.; Klotz, I. M.; Williams, R. J. P. *Arch. Biochem. Biophys.* **1969**, *135*, 419.

(47) Okamura, M. Y.; Klotz, I. M.; Johnson, C. E.; Winter, M. R. C.; Williams, R. J. P. *Biochemistry* **1969**, *8*, 1951.

(48) Dawson, J. W.; Gray, H. B.; Hoenig, H. E.; Rossmann, G. R.; Schredder, J. M.; Wang, R. H. *Biochemistry* **1972**, *11*, 461.

Supplementary Material Available: Listings of crystal data and structure refinement information (Table SI), distances and angles for non-hydrogen atoms (Tables SVIII and SX), anisotropic temperature factors (Tables SII and SV), atomic coordinates and thermal parameters for anions and solvent molecules (Tables SIII and SVI), and hydrogen atom coordinates and temperature factors (Tables SIV and SVII) and figures showing atom numbering for cations and unit cell and packing diagrams (21 pages); tables of observed and calculated structure factors (Tables SXI and SXII) (20 pages). Ordering information is given on any current masthead page.

Contribution from the Department of Chemistry,
The Pennsylvania State University, University Park, Pennsylvania 16802

Spectroscopic Characterization of a Series of Europium(III) Amino Phosphonate Complexes in Solution

Richard C. Holz, Gretchen E. Meister, and William DeW. Horrocks, Jr.*

Received October 11, 1989

The Eu^{3+} complexes of nitrilotris(methylenephosphonic acid) (ntp), ethylenediaminetetrakis(methylenephosphonic acid) (edtp), hexamethylenediaminetetrakis(methylenephosphonic acid) (hdtp), and diethylenetriaminepentakis(methylenephosphonic acid) (dtpp) have been characterized in solution by laser-induced Eu^{3+} luminescence spectroscopy. The latter three ligands form both 2:1 and 1:1 metal-ligand complexes, while ntp forms both 1:1 and 1:2 complexes at pH 6.0. The number of water molecules directly coordinating the metal ion was determined for each complex. The $^7F_0 \rightarrow {}^5D_0$ excitation spectra of edtp, hdtp, and dtpp reveal isomeric forms for both the 2:1 and 1:1 complexes while ntp exhibits only single species for both the 1:1 and 1:2 complexes. Marked changes were observed in the Eu^{3+} $^7F_0 \rightarrow {}^5D_0$ excitation spectra of the various species as a function of pH. The temperature dependence of the excited state lifetime of the Eu^{3+}-edtp system has an activation energy of 5150 cm^{-1}, corresponding to a ligand level this far above the $^5D_0$ state, which is involved in the deexcitation process.

Introduction

The chelating ability of amino phosphonic acids has received considerable attention due to the diverse binding abilities of the phosphonate group.[1-7] Amino phosphonates have been used commercially as herbicides and sequestering agents.[8] Other potential applications include NMR imaging agents, anticorrosive agents, and metal ion separation reagents.[9,10] These ligands can also be thought of as simple models for biologically important phosphonate-containing molecules;[11] moreover, they are structural analogues of the well-known amino carboxylates. However amino phosphonic acids exhibit very different protonation and complexation properties from their aminocarboxylic acid counterparts. These differences stem from the strong pH dependence of complex formation, added bulkiness, and bidentate coordination ability of the phosphonate group, as well as their potential for formation of polymeric species.[11-14]

In order to assess the potential uses and functions of amino phosphonic acids, an understanding of the types of metal complexes formed in solution is required. The use of lanthanide luminescence spectroscopy to probe the solution complexation properties of coordination complexes and biological systems has proven to be particularly informative.[15-17] The ability of certain lanthanide ions to luminesce in solution at room temperature allows a broad amount of structural information to be obtained. Eu^{3+} and Tb^{3+} have been utilized extensively as structural probes in luminescence studies; however, Eu^{3+} is the more desirable owing to its nondegenerate ground ($^7F_0$) and first excited ($^5D_0$) states. Since neither

Chart I. Schematic Representation of the Four Amino Phosphonate Ligands Studied

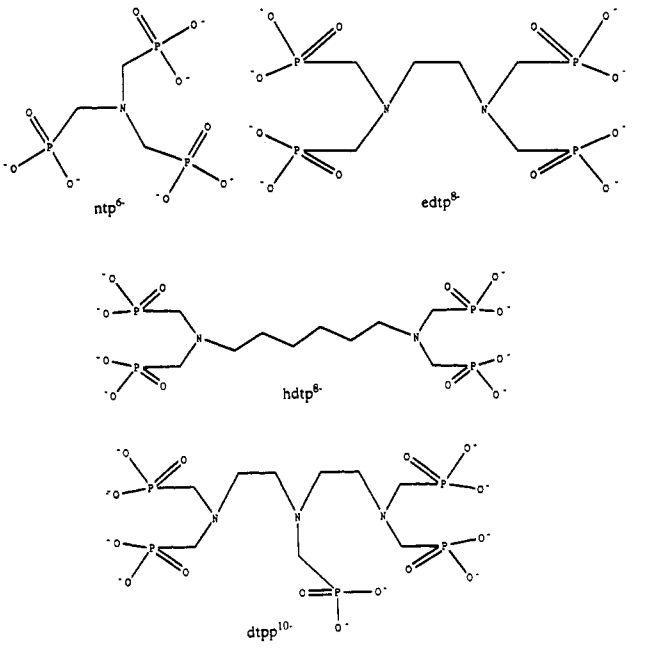

(1) Schwarzenbach, G.; Ackermann, H.; Ruchstuhl, P. *Helv. Chim. Acta* **1949**, *32*, 1175.
(2) Westerback, S.: Martell, A. E. *Nature* **1956**, *178*, 321.
(3) Westerback, S.; Rajan, K. S.; Martell, A. E. *J. Am. Chem. Soc.* **1965**, *87*, 2567.
(4) Motekaitis, R. J.; Murase, I.; Martell, A. E. *Inorg. Chem.* **1976**, *15*, 2303.
(5) Kabachnik, M. I.; Dyatlova, I. M.; Medved', T. A.; Belugin, Yu. F.; Sidorenko, V. V. *Dokl. Chem. Proc. Acad. Sci. USSR* **1967**, *175*, 621.
(6) Rizkalla, E. N.; Zaki, M. T. M. *Talanta* **1979**, *26*, 507.
(7) Zaki, M. T. M.; Rizkalla, E. N. *Talanta* **1980**, *27*, 709.
(8) Smith, P. H.; Raymond, K. N. *Inorg. Chem.* **1988**, *27*, 1056.
(9) Sherry, A. D.; Geraldes, C. F. G. C.; Cacheris, W. P. *Inorg. Chim. Acta* **1987**, *139*, 137.
(10) Sherry, A. D.; Malloy, C. R.; Jeffery, F. M. H.; Cacheris, W. P.; Geraldes, C. F. G. C. *J. Magn. Reson.* **1988**, *76*, 528.
(11) Kabachnik, M. I.; Medved', T. A.; Dyatlov, N. M.; Arkhipova, O. G.; Rudomino, M. V. *Russ. Chem. Rev. (Engl. Transl.)* **1968**, *37*, 503.
(12) Sawada, K.; Araki, T.; Suzuki, T. *Inorg. Chem.* **1987**, *26*, 1199.
(13) Tananaev, I. V.; Tereshin, G. S.; Kuznetsova, O. B.; Beresnev, E. N.; Goeva, L. V. *Russ. J. Inorg. Chem. (Engl. Transl.)* **1981**, *26*, 149.
(14) Tananaev, I. V.; Beresnev, E. N.; Tereshin, G. S.; Kuznetsova, O. B.; Goeva, L. V. *Russ. J. Inorg. Chem. (Engl. Transl.)* **1981**, *26*, 151.
(15) Reuben, J. *Handbook on the Physics and Chemistry of Rare Earths*; Gschneidner, K. A., Eyring, L., Eds.; North-Holland: Amsterdam 1979; Vol. 3, p 515.
(16) Horrocks, W. DeW., Jr.; Albin, M. *Prog. Inorg. Chem.* **1984**, *31*, 1.
(17) Horrocks, W. DeW., Jr.; Sudnick, D. R. *Acc. Chem. Res.* **1981**, *14*, 384.

0020-1669/90/1329-5183$02.50/0